Photodecomposition of Peroxides Containing a 1,4-Bis(phenylethynyl)benzene Chromophore

Dmitry E. Polyansky, Evgeny O. Danilov, Sergey V. Voskresensky, Michael A. J. Rodgers, and Douglas C. Neckers*

Center for Photochemical Sciences,[1] Bowling Green State University, Bowling Green, Ohio 43403

Received: September 8, 2005; In Final Form: February 21, 2006

The photodecomposition dynamics of 1,4-bis(2-[4-*tert*-butylperoxycarbonylphenyl]ethynyl)benzene (**1**) have been compared with those of model compounds in the picosecond and nanosecond time domains by various photophysical techniques. Ultrafast visible transient absorption spectrometry revealed the singlet excited state of 1,4-bis(4-phenylethynyl)benzene (BPB) depopulates radiatively with a rate of 1.75×10^9 s^{-1} and 95% efficiency. Phenyl ester moieties attached to the BPB core accelerate intersystem crossing ($k = 2.8 \times 10^8$ s^{-1}) and reduce the fluorescence quantum yield ($\Phi_{FL} = 0.82$). The peroxide oxygen−oxygen bond of **1** cleaves ($k = 3.6 \times 10^{11}$ s^{-1}) directly from the singlet excited state (60% efficiency) causing a highly reduced fluorescence yield and leading to formation of aroyloxyl radicals. The next reaction step involves decarboxylation of the aroyloxyl radicals. Transient absorption signals in the MID IR region correspond to CO_2 with the formation rate (2.5×10^6 s^{-1}) as measured by nanosecond transient IR experiments. The transient IR spectra of the excited state of BPB, as well as of the aroyloxyl radical, evidenced a red shift in the acetylene triple bond absorption indicative of a decrease in the bond order. This clearly shows that delocalization of excitation energy over the BPB chromophore induces significant structural changes. The proposed mechanism is based on the rates of photophysical and photochemical channels and involves an additional population channel of the BPB triplet excited state from the upper singlet states.

Introduction

Oligo(phenylethynyl) fragments successfully integrated into rigid molecular structures offer unusual properties in both the solid state and solution. These properties, when incorporated into materials, have contributed to a number of new applications of organic compounds. Compounds based on a phenylene−ethynylene chromophore have been used to synthesize new efficient light absorbers and emitters[2] as well as highly conjugated molecular wires targeting an efficient energy or charge transfer.[3] The ability to delocalize charge over significant distance suggests that derivatized oligo(phenylethynyl) compounds are good candidates for nonlinear optical (NLO) materials.[4,5] The use of the alkynyl function in new materials has, in some ways, proceeded more rapidly than our understanding of how electron density is transmitted through these molecular architectures. The current study addresses this through a characterization of excited-state behavior in several compounds with extended phenylethynyl chromophores.

Previous studies on the nature the excited states of molecules with extended phenylethynyl chromophores are mostly limited to data on fluorescence dynamics and theoretical models that provide little insight to fundamental photophysics of these compounds.[6,7] Recent results demonstrated the importance of time-resolved experiments to describe photophysical behavior of oligo(phenylethynyl) compounds and even disagreed with some results obtained previously from steady-state experiments.[8] This fact inspired more detailed time-resolved studies using various transient techniques in wide temporal and spectral ranges.

* To whom correspondence should be addressed. E-mail: neckers@photo.bgsu.edu.

Previous studies have demonstrated that higher excited states of oligo(phenylethynyl) compounds possess some degree of cumulenic structure,[8,9] suggesting the redistribution of electron density significant enough to cause a change in the bond order. We report investigations on the influence of an unpaired electron coupled directly to 1,4-bis(phenylethynyl)benzene chromophore on the electronic structure of the central phenylethynyl core and the possible influence of the highly conjugated system on the delocalization of the unpaired electron along the conjugated backbone of the molecule. For such studies the peroxy ester functionalized 1,4-bis(phenylethynyl)benzene is an ideal candidate since the decomposition of peroxy esters commonly proceeds through facile cleavage of the −O−O− bond leading to the formation of corresponding aroyloxyl radical followed by decarboxylation and the formation of aryl radical and carbon dioxide.[10] Reaction rates lying in the range from several picoseconds[11,12] to tens of microseconds,[13] as well as a high IR extinction coefficient and distinct peak position of carbonyl vibration, make most of the intermediates observable if one uses a majority of the now available time-resolved techniques.

In this study, we report on a new class of peroxy ester-substituted phenylethynyl compounds studied by time-resolved UV−vis (TRUV) and time-resolved FTIR (TRIR) spectrometry. The spectroscopic studies together with a photostationary product analysis allowed for elucidating of the mechanism of peroxide photodecomposition and the nature of the transient species involved therein.

Experimental Section

General Methods. ^1H and ^{13}C NMR spectra were recorded on Bruker Avance 300 MHz system. Chemical shifts are in ppm with TMS as the internal standard. GC-MS and DIP mass

10.1021/jp055078m CCC: $33.50
Published on Web 03/30/2006

spectra were measured on a Shimadzu GC/MS-QP5050A spectrometer. Melting points were determined with a Fisher-Johns melting point apparatus and are uncorrected. Elemental analysis was performed by Atlantic Microlab, Inc. HPLC measurements were performed on Hitachi LC-7000 series instrument equipped with an Alltech Nucleosil C18 column. UV−vis spectra were measured with Shimadzu UV-2401PC spectrophotometer. Photodecomposition quantum yields were obtained by the direct irradiation of samples with an Omnichrome Series 74XA HeCd laser (325 nm) interrupted with a Uniblitz SD-10 shutter drive timer. IR-ATR spectra of solid samples were measured on a Thermo Nicolet IR200 ATR equipped spectrometer. The fluorescence quantum yields were obtained against standard solutions of 2-aminopyridine in 0.1 N sulfuric acid[14] or anthracene in ethanol.[15]

Materials. All spectroscopic samples were thoroughly dried, and their purity was verified by HPLC. All solvents, either for reactions or spectroscopic measurements, were dried via distillation over an appropriate drying agent according to standard procedures.[16] The following chemicals were commercially available and were used as received: 1-ethynyl-4-bromobenzene (Acros); 4-iodobenzoic acid (Acros); copper(I) iodide (Aldrich); terephthaldehyde (Acros); 3-methyl-3-butyn-2-ol (Acros); $PdCl_2(PPh_3)_2$ (Aldrich); *n*-butyllithium (2.5 M in hexanes) (Aldrich). Aldrich silica gel 60 Å (70−270 mesh) was used in chromatography.

Nanosecond Infrared Time-Resolved Experiments. The **t**ime-resolved FTIR setup has been described elsewhere.[17] Briefly, the third harmonic of a Spectra Physics YAG:Nd^{3+} laser (354.7 nm) was used as an excitation source in all experiments. The laser was operated in a pulsed mode with a repetition rate of 10 Hz and the energy varied from 1.5 to 5 mJ/pulse. The sample solutions (chloroform was used as a solvent in all experiments) were pumped through a 1 mm thick CaF_2 flow cell with a flow rate of up to 150 mL/min. All spectra were recorded in a 1500−2800 cm^{-1} spectral window with resolution 8 cm^{-1} every 20 ns. The raw data were processed and visualized with custom written LabView-based software.

Nanosecond UV−Vis Time-Resolved Experiments. The detailed description of the time-resolved UV−vis spectrometer is available elsewhere.[18] Briefly, the third harmonic of a Continuum YAG:Nd^{3+} laser (354.7 nm) was used as an excitation source in all experiments. The laser was operated with a repetition rate of 5 Hz, and the energy was kept between 0.5 and 3 mJ/pulse. Solutions (chloroform was used as a solvent in all experiments) were pumped through a quartz flow cell with three polished windows and with a flow rate of up to 150 mL/min. Transient UV−vis spectra were acquired every 10 nm in a 330−820 nm spectral interval.

Ultrafast VIS Time-Resolved Experiments. A detailed description of the home-built ultrafast VIS setup is available elsewhere.[19] Briefly, frequency converted (340 nm) output from Spectra-Physics Hurricane femtosecond laser was used for excitation. Probe pulses were generated in a CaF_2 crystal and overlapped with the pump inside a sample flow cell. The solution (chloroform was used as a solvent in all experiments) was degassed with Ar to avoid the formation of long-lived intermediates (over 1 ms) and pumped through a 2 mm thick CaF_2 flow cell with the flow rate of up to 150 mL/min. The absorption of the sample at the excitation wavelength was 0.8−1.0 (2 mm cell) and was constantly checked to ensure that the decomposition of the starting material was less than 10%.

DFT Calculations. DFT calculations were done using the Gaussian 98 package.[20] The geometries were optimized using the B3LYP level of theory with the 6-31G(d) basis set in a vacuum. IR frequencies were calculated on optimized structures using the same basis set. All frequencies reported were scaled up by a factor of 0.96, which is traditionally used for this size of basis set in DFT calculations.[21]

Synthesis. 1,4-Bis(2,2-dibromovinyl)benzene. 1,4-Bis(2,2-dibromovinyl)benzene was synthesized according to the Corey and Fuchs method[23] with a modification of the separation step. The precipitated triphenylphosphine oxide was filtered out and washed with a hexane/CH_2Cl_2 (1:1) mixture, and the combined organic solutions were concentrated under reduced pressure. The resulting residue was recrystallized from EtOH affording 86% yield of pure product, mp 97−98 °C (lit. mp 98−99 °C).[24] EI-MS (70 eV): *m*/*z* 446 (M^+, 4 Br), 286 (2 Br), 206, 144, 126, 103.

1,4-Diethynylbenzene. A solution of 1,4-bis(2,2-dibromovinyl)benzene (188.7 g, 0.42 mol) in dry THF (500 mL) was added dropwise to a solution of *n*-BuLi (694 mL as a 2.5 M solution in hexane, 1.72 mol) in dry THF (700 mL) at −78 °C for 1.5 h. Then the reaction was brought slowly to rt (room temperarure), stirred for 12 h, and quenched with ice/water mixture. The organic layer was isolated and dried over Na_2SO_4, and solvent was removed under reduced pressure. The resulting residue was passed through a small amount of silica gel using hexane as an eluent providing pure product in 99% (52.9 g) yield. Mp: 96 °C (lit. mp 95 °C).[25] EI-MS (70 eV): *m*/*z* 126 (M^+), 100, 98, 87, 76, 74, 63, 50.

General Procedure for Preparation of Symmetric 1,4-Bis-(2-[4-X-phenyl]ethynyl)benzenes by Sonogashira Coupling between 1,4-Diethynylbenzene and 4-Iodoarenes. To a carefully degassed solution of the appropriate 4-iodoarene (79.3 mmol), PPh_3 (207 mg, 0.79 mmol, 2%), and $PdCl_2(PPh_3)_2$ (167 mg, 0.24 mmol, 0.6%) in 80 mL of dry THF and 40 mL of dry triethylamine was added CuI (150 mg, 0.79 mmol, 2%). The resulting mixture was degassed for 5 min, and a solution of 1,4-diethynylbenzene (5 g, 39.6 mmol) in 20 mL of dry THF was added during 5 min via syringe. The reaction was stirred overnight at 50 °C under nitrogen atmosphere. The resulting precipitate was filtered out, washed with THF (2 × 20 mL) and 5% NH_4Cl (100 mL), and then air-dried to provide pure product.

1,4-Bis(4-tolylethynyl)benzene (4) was prepared according to the general procedure described above using 4-iodotoluene in 84% yield (10.2 g). EI-MS (70 eV): *m*/*z* 307 ($M^+ + 1$), 306 (M^+), 290, 289, 263, 153, 145, 126. Mp: 218−219 °C (lit. mp 216 °C).[26] Principle IR bands (solid, ATR, cm^{-1}): 3027 (w), 2922 (w), 2860 (w), 1521 (s), 1410 (w), 1306 (w), 1265 (w), 1212 (w), 1192 (w), 1121 (w), 1110 (w), 1035 (w), 1017 (w), 950 (w), 840 (s), 810 (s), 762 (w), 740 (w), 704 (w), 647 (w).

1,4-Bis(2-[4-carboxyphenyl]ethynyl)benzene was prepared according to the general procedure in 90% yield (13.1 g) using 4-iodobenzoic acid. Mp: >300 °C (dec). EI-MS (70 eV): *m*/*z* 366 (M^+), 349, 321, 276, 274, 183, 166, 152, 138. Principle IR bands (solid, ATR, cm^{-1}): 2840 (m, br), 1678 (s), 1603 (s), 1556 (m), 1518 (w), 1490 (w), 1420 (s), 1314 (s), 1279 (s), 1174 (s), 1100 (m), 1014 (m), 937 (m), 860 (s), 834 (s), 770 (s), 692 (s).

1,4-Bis(2-[4-phenyloxycarbonylphenyl]ethynyl)benzene (3) was prepared according to the general procedure in 85% yield (17.5 g) using phenyl 4-iodobenzoate. EI-MS (70 eV): *m*/*z* 518 (M^+), 425, 304, 274, 207, 166. Anal. Calcd for $C_{36}H_{22}O_4$: C, 83.38; H, 4.28. Found: C, 83.40; H, 4.07. Mp: 250−251 °C (dec). Principle IR bands (solid, ATR, cm^{-1}): 3070 (w), 3047

(w), 1737 (s), 1590 (m), 1560 (w), 1518 (w), 1484 (m), 1402 (m), 1265 (m), 1212 (m), 1176 (w), 1160 (m), 1145 (m), 1063 (s), 1012 (m), 1000 (m), 912 (m), 854 (s), 840 (s), 754 (s), 738 (s), 685 (s).

1,4-Bis(2-[4-*tert*-butylperoxycarbonylphenyl]ethynyl)-benzene (1). A mixture of 1,4-bis(2-[4-carboxyphenyl]ethynyl)-benzene (7.7 g, 21.0 mmol), pyridine (3.32 g, 42.1 mmol), and oxalyl chloride (8 g, 63.0 mmol) in 100 mL of dry CH_2Cl_2 was stirred for 24 h at ambient temperature. After that the reaction was concentrated to dryness under reduced pressure to provide **1,4-bis(2-[4-chlorocarbonylphenyl]ethynyl)benzene**, which was sufficiently pure for the next step. EI-MS (70 eV): *m*/*z* 402 (M^+, 2 Cl), 367 (1 Cl), 304, 276, 274, 166, 152, 138, 125, 112, 100.

The residue (above) was dissolved in dry CH_2Cl_2 (60 mL) and cooled to 0 °C, and a solution of *tert*-butyl peroxide (6.1 g of 5−6 M solution in decane, 67.3 mmol) and pyridine (6.7 g, 84.7 mmol) in dry CH_2Cl_2 (30 mL) was added dropwise during 15 min under argon. The reaction mixture was stirred for 4 h on an ice/water bath and then was left overnight. After that the reaction mixture was washed sequentially with cold water and 5% $NaHCO_3$, dried over Na_2SO_4, and concentrated under reduced pressure. The residue was passed through a small layer of silica gel using a mixture of hexane/CH_2Cl_2 (1:1) as an eluent, the solvents were evaporated under vacuum, and the crude product was dissolved in 25 mL of dry CH_2Cl_2. The slow addition of 60 mL of hexane afforded the precipitation of pure product, which was filtered off, washed with hexane, and vacuum-dried. Yield: 47% (5.0 g). EI-MS (70 eV): *m*/*z* 510 (M^+), 421 ($M^+ - t$-BuOO), 366, 349, 322, 304, 276, 166, 152, 138. Anal. Calcd for $C_{32}H_{30}O_6$: C, 75.28; H, 5.92. Found: C, 75.47; H, 5.86. ^{1}H NMR (300 MHz, CD_2Cl_2): δ 7.9 (d, J = 8.7 Hz, 4H), 7.6 (d, J = 8.7 Hz, 4H), 7.6 (s, 4H), 1.4 (s, 18H). ^{13}C NMR (50 MHz, $CDCl_3$): δ 163.8, 131.7, 129.1, 128.1, 127.1, 122.9, 92.2, 90.5, 84.1, 26.3. Principle IR bands (solid, ATR, cm^{-1}): 2980 (m), 2930 (w), 2212 (w), 1750 (s), 1600 (s), 1516 (m), 1476 (w), 1408 (m), 1386 (w), 1364 (m), 1309 (w), 1284 (w), 1231 (s), 1192 (s), 1174 (s), 1144 (s), 1050 (s), 1030 (s), 1012 (s), 870 (m), 844 (s), 830 (s), 757 (s), 670 (s).

Ethyl 4-[2-(4-Bromophenyl)-1-ethynyl]benzoate (2a). To a degassed solution of ethyl 4-iodobenzoate (15.0 g, 54.3 mmol) and $PdCl_2(PPh_3)_2$ (133 mg, 0.19 mmol, 0.35%) in 100 mL of dry THF and 50 mL of dry triethylamine was added CuI (103 mg, 0.54 mmol, 1%). The resulting mixture was degassed for 5 min, and a solution of 1-ethynyl-4-bromobenzene (9.8 g, 54.3 mmol) in 15 mL of dry THF was added dropwise for 15 min. After the addition was complete, the reaction mixture was stirred overnight at 45−50 °C. Then the reaction mixture was concentrated to dryness under reduced pressure and the residue passed through a small layer of silica gel using CH_2Cl_2 as an eluent. Recrystallization from ethyl alcohol yielded 16.1 g (90%) of pure product, Mp: 112−113 °C. ^{1}H NMR (300 MHz, $CDCl_3$): δ 8.03 (AA′BB′, apparent d, J = 8.4 Hz, 2H), 7.57 (AA′BB′, apparent d, J = 8.4 Hz, 2H), 7.50 (AA′BB′, apparent d, J = 8.7 Hz, 2H), 7.40 (AA′BB′, apparent d, J = 8.7 Hz, 2H), 4.38 (q, J = 7.2 Hz, 2H), 1.40 (t, J = 7.2 Hz, 3H). ^{13}C NMR (75 MHz, $CDCl_3$): δ 165.9, 133.1, 131.8, 131.7, 131.4, 130.1, 129.5, 127.4, 123.0, 121.7, 91.1, 89.8, 65.6, 61.1, 14.3. Principle IR bands (solid, ATR, cm^{-1}): 2985 (w), 2210 (w), 1711 (s), 1604 (s), 1511 (m), 1480 (m), 1450 (m), 1400 (w), 1385 (w), 1365 (s), 1267 (s), 1160 (m), 1090 (s), 1067 (m), 1002 (s), 855 (s), 818 (s), 760 (s), 694 (s).

Ethyl 4-{2-[4-(3-Hydroxy-3-methyl-1-butynyl)phenyl]-1-ethynyl}benzoate (2b). A two-neck 300 mL round-bottom flask was charged with ethyl ester **2a** (10.5 g, 31.9 mmol), PPh_3 (418 mg, 1.6 mmol, 5%), $PdCl_2(PPh_3)_2$ (358 mg, 0.51 mmol, 1.6%), 140 mL of the dry Et_3N, and 70 mL of the pyridine. To the resulting degassed suspension was added CuI (474 mg, 2.5 mmol, 7.8%) followed by the addition of 3-methyl-3-butyn-2-ol (3.5 g, 41.6 mmol). The reaction mixture was stirred under nitrogen for 4 days under reflux. The reaction was monitored by GC/MS. After each day a fresh portion of 3-methyl-3-butyn-2-ol (3.5 g, 41.6 mmol) was added to ensure complete conversion of the starting material. The solvents were then evaporated under reduced pressure, the residue was dissolved in a minimal amount of toluene, and the product was precipitated by addition of a 2-fold excess of hexane. The product was filtered off, dissolved in a minimal amount of CH_2Cl_2, and passed twice through a small amount of the silica gel using CH_2Cl_2 as an eluent. After that solvent was evaporated under reduced pressure to afford 9.2 g (87%) of the pure alcohol. Mp: 128−129 °C. ^{1}H NMR (300 MHz, $CDCl_3$): δ 8.03 (AA′BB′, apparent d, J = 8.4 Hz, 2H), 7.58 (AA′BB′, apparent d, J = 8.7 Hz, 2H), 7.48 (AA′BB′, apparent d, J = 8.7 Hz, 2H), 7.41 (AA′BB′, apparent d, J = 8.4 Hz, 2H), 4.39 (q, J = 7.2 Hz, 2H), 2.04 (br s, 1H), 1.41 (t, J = 7.2 Hz, 3H). ^{13}C NMR (75 MHz, $CDCl_3$): δ 166.0, 131.6, 131.5, 131.4, 130.0, 129.5, 127.6, 123.2, 122.5, 96.0, 91.8, 90.3, 81.7, 65.6, 61.1, 31.4, 14.3. Principle IR bands (solid, ATR, cm^{-1}): 3360 (w), 2985 (w), 1710 (s), 1596 (m), 1512 (m), 1466 (m), 1406 (m), 1364 (m), 1267 (s), 1150 (s), 1098 (s), 1016 (m), 960 (m), 860 (s), 840 (s), 764 (s), 697 (s).

4-{2-[4-(1-Ethynyl)phenyl]-1-ethynyl}benzoic Acid (2c). A mixture of ethyl 4-{2-[4-(3-hydroxy-3-methyl-1-butynyl)-phenyl]-1-ethynyl}benzoate (4.9 g, 14.7 mmol), 3.4 g of KOH, and 50 mL of *n*-BuOH was stirred for 2 h under reflux conditions. The reaction was then cooled to ambient temperature, and the resulting precipitate was filtered out, washed with water and cold EtOH, and vacuum-dried to provide 4.2 g (100%) of the pure potassium salt of **2c**, which upon acidification with 2 N HCl provided the corresponding carboxylic acid. ^{1}H NMR (300 MHz, DMSO-d_6): δ 7.97 (d, J = 8.4 Hz, 2H), 7.65 (J = 8.7 Hz, 2H), 7.60 (AA′BB′, apparent d, J = 8.4 Hz, 2H), 7.54 (AA′BB′, apparent d, J = 8.4 Hz, 2H), 4.40 (s, 1H). EI-MS (70 eV): *m*/*z* 246 (M^+), 229, 200, 174, 150. Principle IR bands (solid, ATR, cm^{-1}): 3270 (s), 2821 (m, br), 1673 (s), 1605 (s), 1580 (w), 1560 (w), 1536 (w), 1490 (w), 1425 (m), 1404 (m), 1318 (m), 1280 (s), 1172 (m), 1100 (m), 1015 (m), 930 (m), 857 (m), 830 (s), 770 (s), 690 (m).

Phenyl 4-{2-[4-(1-Ethynyl)phenyl]-1-ethynyl}benzoate (2d). A stirred suspension of the potassium salt of **2c** (4.0 g, 14.1 mmol) in 70 mL of dry CH_2Cl_2 was cooled on the ice bath, and oxalyl chloride (3.8 g, 30 mmol) was added. One drop of DMF was added to initiate the reaction. The mixture was stirred for 1 h at 5 °C, the cooling bath removed, and stirring continued for 1 h at ambient temperature. The reaction mixture was concentrated until dryness under reduced pressure, and the residue was dissolved in 100 mL of dry CH_2Cl_2 with the solution cooled on an ice bath. A solution of phenol (3.8 g, 40 mmol) and pyridine (3.2 g, 40 mmol) in 15 mL of dry CH_2Cl_2 was added dropwise over 30 min. The reaction was then stirred for 2 h at 5 °C and left at room-temperature overnight. The resulting solution was quenched with ice/water, and the organic layer was separated, dried over Na_2SO_4, and passed through a small amount of silica gel using CH_2Cl_2 as an eluent. Recrystallization from the acetone/hexane (1:2) system yielded 2.7 g (59%) of pure ester. ^{1}H NMR (300 MHz, $CDCl_3$): δ 8.17 (AA′BB′, apparent d, J = 8.1 Hz, 2H), 7.78 (AA′BB′, apparent d, J =

8.4 Hz, 2H), 7.63 (AA′BB′, apparent d, $J = 8.47$ Hz, 2H), 7.55 (AA′BB′, apparent d, $J = 8.1$ Hz, 2H), 7.48 (m, 2H), 7.31 (m, 2H), 7.60 (AA′BB′, apparent d, $J = 8.4$ Hz, 2H), 7.54 (AA′BB′, apparent d, $J = 8.4$ Hz, 2H), 4.39 (s, 1H). EI-MS (70 eV): *m*/*z* 322 (M^+), 229, 200, 174, 150, 100. Principle IR bands (solid, ATR, cm^{-1}): 3270 (s), 3066 (w), 3040 (w), 1740 (s), 1590 (m), 1490 (m), 1400 (m), 1265 (m), 1212 (m), 1160 (w), 1068 (s), 1015 (m), 998 (m), 912 (m), 855 (m), 837 (s), 758 (s), 735 (s), 685 (s), 642 (m), 623 (m).

4-(2-{4-[2-(4-Phenyloxycarbonylphenyl)-1-ethynyl]phenyl}-1-ethynyl)benzoic Acid (2e). To a carefully degassed mixture of 4-iodobenzoic acid (1.7 g, 6.9 mmol), PPh_3 (16 mg, 0.06 mmol, 1%), $PdCl_2(PPh_3)_2$ (44 mg, 0.06 mmol, 1%), 35 mL of the dry Et_3N, and 80 mL of the dry THF was added CuI (71 mg, 0.037 mmol, 6%). The resulting mixture was degassed for 5 min, and a solution of phenyl ester (2 g, 6.2 mmol) in 10 mL of dry THF was added dropwise during several minutes. The reaction was stirred overnight at 50 °C, and the resulting precipitate was filtered out, washed sequentially with THF (2 × 20 mL) and 5% NH_4Cl (100 mL), and then vacuum-dried to provide 2.1 g (77%) of the pure product. Principle IR bands (solid ATR, cm^{-1}): 3030 (m, br), 1740 (s), 1700 (w), 1590 (m), 1490 (m), 1400 (s), 1266 (s), 1215 (s), 1176 (s), 1158 (s), 1072 (s), 835 (s), 760 (s), 690 (s).

***tert*-Butyl 4-(2-{4-[2-(4-phenyloxycarbonylphenyl)-1-ethynyl]phenyl}-1-ethynyl)peroxybenzoate (2).** The mixture of acid **2e** (0.5 g, 1.1 mmol), pyridine (0.11 g, 1.4 mmol), and oxalyl chloride (0.16 g, 1.3 mmol) in 100 mL of dry CH_2Cl_2 was stirred for 24 h at ambient temperature. After that the reaction was concentrated to dryness under reduced pressure to provide 4-(2-{4-[2-(4-phenyloxycarbonylphenyl)-1-ethynyl]-phenyl}-1-ethynyl)benzoyl chloride (**2f**), which was sufficiently pure for the next step.

The residue from the previous step was dissolved in dry CH_2Cl_2 (50 mL) and cooled to 0 °C, and a solution of *tert*-butyl peroxide (0.34 mL of 5−6 M solution in decane, 1.9 mmol) and pyridine (0.14 mL, 1.7 mmol) in dry CH_2Cl_2 (30 mL) was added dropwise over 15 min under argon atmosphere. The reaction mixture was stirred for 4 h on the ice/water bath and left overnight on a cold water bath. After that the reaction mixture was washed with cold water and 5% $NaHCO_3$, dried over Na_2SO_4, and concentrated under reduced pressure. The concentrated solution was flash-chromatographed through silica gel using a hexane/CH_2Cl_2 gradient mixture as an eluent affording pure product in 27% yield (0.15 g). Anal. Calcd for $C_{34}H_{26}O_5$: C, 79.36; H, 5.09. Found: C, 79.34; H, 4.98. ^{1}H NMR (300 MHz, $CDCl_3$): δ 8.2 (d, $J = 8.7$ Hz, 2H), 7.95 (d, $J = 8.7$ Hz, 2H), 7.7 (d, $J = 8.7$ Hz, 2H), 7.65 (d, $J = 8.7$ Hz, 2H), 7.59 (s, 4H), 7.46 (t, $J = 7.5$ Hz, 2H), 7.31 (t, $J = 7.5$ Hz, 1H), 7.24 (d, $J = 7.5$ Hz, 2H). ^{13}C NMR (75 MHz, $CDCl_3$): δ 164.2, 163.3, 150.8, 131.52, 131.46, 131.43, 129.8, 129.2, 129.0, 128.8, 128.0, 127.8, 127.1, 125.7, 122.8, 122.7, 121.4, 91.83, 91.78, 90.2, 90.1, 83.7, 25.7. Principle IR bands (solid, ATR, cm^{-1}): 2980 (w), 2933 (w), 2220 (w), 1750 (s), 1733 (s), 1600 (m), 1520 (w), 1490 (m), 1400 (m), 1366 (m), 1260 (s), 1230 (s), 1190 (s), 1176 (s), 1050 (s), 1015 (s), 910 (w), 850 (s), 837 (s), 755 (s), 745 (s), 727 (s), 687 (s).

Results

Steady-State Photolysis and Fluorescence Experiments. The structures of compounds studied are shown in Chart 1. The photolysis of **1** in carbon tetrachloride led exclusively to the formation of 1,4-bis(4-chlorophenylethynyl)benzene, while the major photochemical product of photodecomposition of **1** in benzene was 1,4-bis(4-phenyl phenylethynyl)benzene. The infrared spectra of 350 nm irradiated solutions of **1** ($\Phi_d = 0.6$) and **2** in chloroform showed depletion of the ground-state absorption in the carbonyl region and the formation of an intense band at 2335 cm^{-1} attributed to carbon dioxide (Figure S1 in Supporting Information). Optically dilute solutions of **1**, **3**, and **4** in chloroform were used to measure fluorescence quantum yields. The values of Φ_{FL} were 0.95 ± 0.05 for **4**, 0.82 ± 0.05 for **3**, and ∼0.03 for **1**.

CHART 1: Structures of the Compounds 1−4

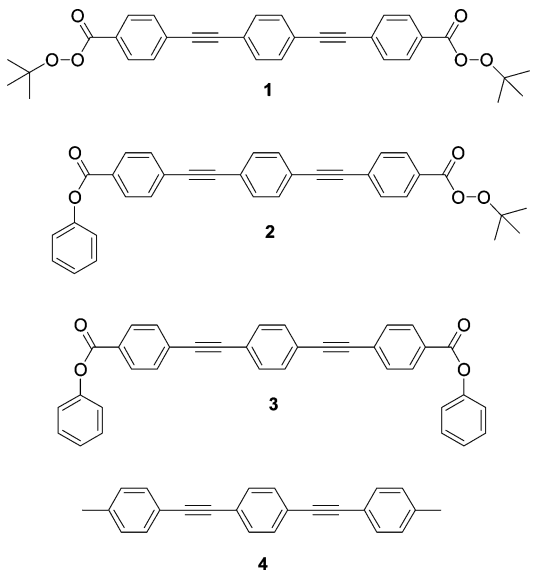

Nanosecond Time-Resolved Infrared Spectra. The transient FTIR (TRIR) spectra of **1** and **2** obtained with nanosecond time resolution are shown in Figure 1. Common features to both are the bleaching of the ground state at 1750 cm^{-1}, the transient band around 2112 cm^{-1}, and the formation of an absorption at 2335 cm^{-1}. Carbon dioxide is one of the anticipated products of peroxy ester decomposition. Intense absorption of CO_2 in $CHCl_3$ appears at 2335 cm^{-1}, unambiguously confirming the origin of the 2335 cm^{-1} band observed after photolysis of **1** and **2**. The origin of the peak at 2112 cm^{-1} will be discussed later.

Negative transient signals in Figure 1 correspond to the ground-state depopulation (bleaching). Immediately after the laser flash at 355 nm with the energy of 1.5 mJ, the bleaching signal at 1755 cm^{-1} in **1** and **2** grew in within the response

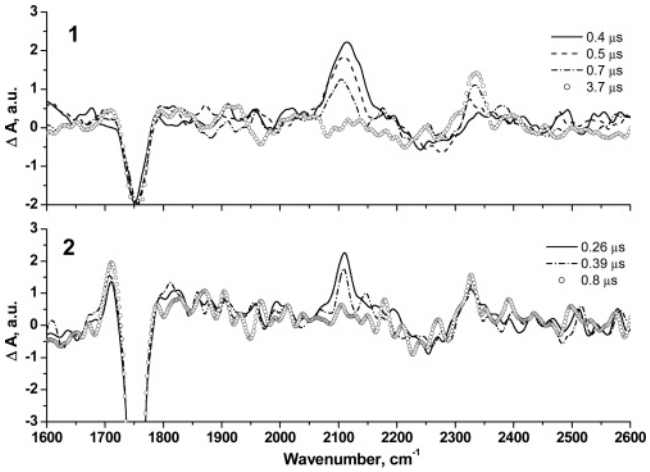

Figure 1. Time evolution of transient FTIR spectra of **1** and **2** acquired after 355 nm laser pulse.

TABLE 1: Kinetics of IR Bands in 1 and 2 Monitored by Time-Resolved Infrared Spectrometry after a 355 nm Laser Pulse

		kinetics of IR bands (ns)			
compd		1710 cm^{-1}	1750 cm^{-1}	2112 cm^{-1}	2335 cm^{-1}
1	formation		<30	<30	400 ± 45
	decay			370 ± 20	
2	formation	186 ± 25	<30	<30	220 ± 20
	decay			170 ± 30	

time of the experimental system and did not recover within the time window of the experiment (ca. 20 μs). This instantaneous, nonrecoverable bleaching signal is consistent with the presence of a fast photochemical channel irreversibly consuming the ground-state population. No ground-state bleaching was observed in the model compound **3** under the same excitation conditions at the laser pulse energy of 1.5 mJ.

The kinetic parameters of the observed IR transients are summarized in Table 1. The in-pulse formation of the 2112 cm^{-1} transient was followed by its decay with a lifetime of 370 ns for compound **1** and 170 ns for **2**. The decay of the 2112 cm^{-1} transient was concomitant with the formation of the 2335 cm^{-1} band corresponding to the absorption of carbon dioxide (see Figure S2 in Supporting Information for kinetics details). The lifetimes and amplitudes of the 2112 cm^{-1} transient were identical in experiments with argon-saturated and oxygen-saturated solutions.

A closer look at the bleaching of ground-state absorption in **2** (Figure 2) and a comparison to its ground-state spectrum (see also Figure S4 in Supporting Information) reveals that only the band corresponding to the absorption of the carbonyl group attached to peroxide moiety is bleached indicating that the peroxy ester moiety of **2** is the only reactive site under the experimental conditions.

To compare the transient behavior of **1** and **2** to the chemically stable model compound **3,** TRIR spectra of **3** after 355 nm laser pulse were recorded. In Figure 3, the transient spectrum of **3** acquired 1 μs after 355 nm laser flash is shown together with the ground-state absorption spectrum. An in-pulse bleaching of the ground-state absorption at 1735 and 1604 cm^{-1} was accompanied by the appearance of transient absorption bands at 1712 and 1580 cm^{-1}. The transient absorption bands decayed with a lifetime similar to that of the recovery of the ground-state bleaching (Table 2).

Nanosecond UV−Vis Transient Absorption Spectrometry. UV−vis transient absorption (TRUV) spectra of **1** and **3** were acquired after a 355 nm laser pulse with nanosecond time resolution (Figure 4). A broad intense band around 550 nm was

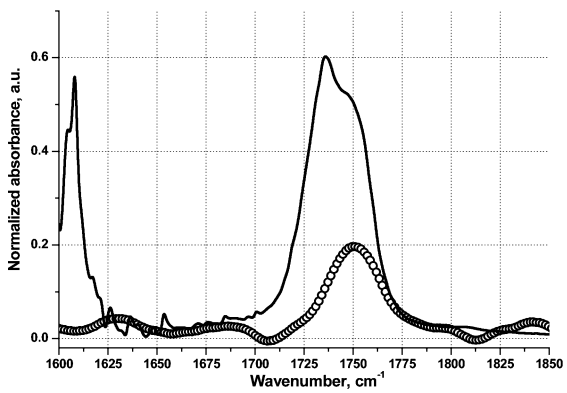

Figure 2. FTIR spectrum of the ground-state absorption of **2** (line) and (inverted) time-resolved FTIR spectrum of the ground-state decay (circles) acquired after 100 ns after the 355 nm laser pulse.

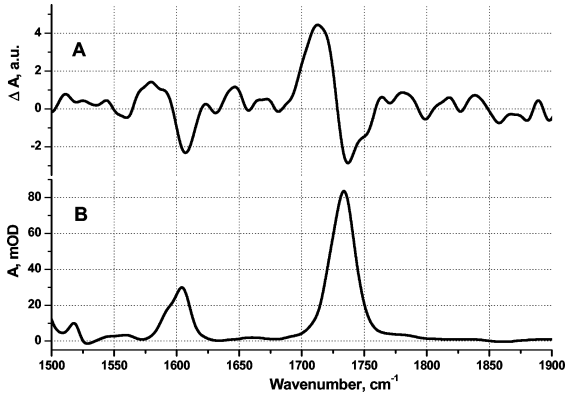

Figure 3. Time-resolved FTIR spectrum of **3** (A) acquired 1 μs after the 355 nm laser pulse and the ground-state absorption spectrum of **3** (B).

TABLE 2: TRIR Data Obtained after Flash Photolysis of 3 with a 355 nm Laser Pulse

transient, cm^{-1}	type	lifetime, μs
1735	recovery of GS bleaching	5.80 ± 0.51
1604	recovery of GS bleaching	5.31 ± 0.92
1712	transient decay	5.15 ± 0.25

TABLE 3: Transient Absorption Maxima and Lifetimes of the Transients Observed after 355 nm Laser Flash Photolysis of 1 and 3

	abs max,	max amplitude,	lifetime, μs	
compd	nm	OD	Ar saturated	O_2 saturated
1	575	0.008	0.35 ± 0.04	0.100 ± 0.003
			21.4 ± 0.4	
3	593	0.065	87.8 ± 1.2	0.099 ± 0.006

observed for both compounds. The wavelengths of the transient absorption maxima and lifetimes of the transients are reported in Table 3. Notably the transient signals observed after the photolysis of **1** decay biexponentially with a short component of 350 ns similar to the decay rate of the 2112 cm^{-1} transient (370 ns) observed in the TRIR experiment. On the other hand, transients observed after the photolysis of model **3** decayed monoexponentially with a lifetime of about 90 μs. The transient absorption lifetimes observed in experiments with **3**, as well as the long component of the transient in the case of **1**, were significantly shortened upon saturation of the solutions with oxygen (Table 3). The short component of the transient absorption decay of **1** was quenched with the addition of radical scavenger acrylonitrile.

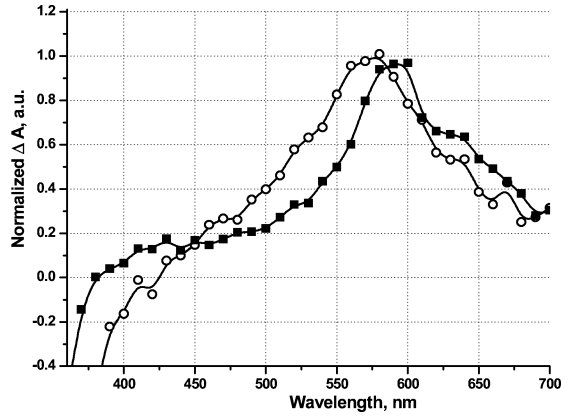

Figure 4. Normalized transient spectra of argon saturated $CHCl_3$ solutions of compounds **1** (open circles) and **3** (solid squares) acquired 3 μs after the 355 nm laser pulse.

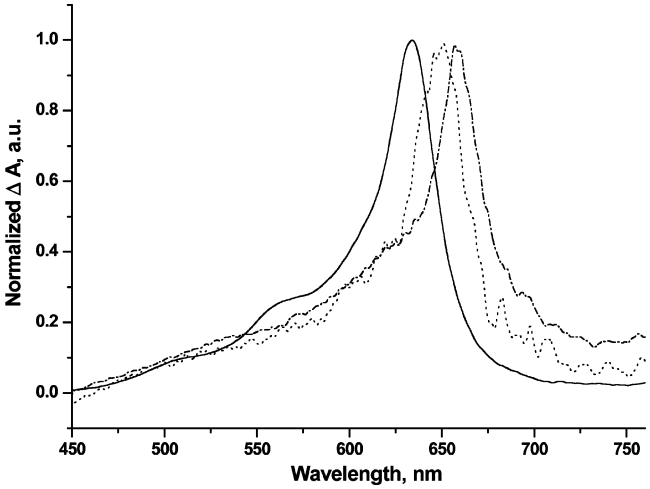

Figure 5. VIS transient spectra of **1** (dot), **3** (dash−dot), and **4** (solid) acquired 2 ps after the 340 nm laser pulse.

TABLE 4: Transient Absorption Maxima and Lifetimes of the Transients Observed in Ultrafast Experiments with 1, 3, and 4

compd	abs max, nm	lifetime, ps
1	650	2.77 ± 0.02
3	658	632 ± 16
4	634	570 ± 44

Ultrafast Spectra. Ultrafast VIS transient absorption spectra of **1**, **3**, and **4** are shown in Figure 5. The common spectroscopic feature for each is a sharp, intense band around 650 nm tailing into the blue region of the spectrum; $\lambda_{max} = 650$ nm for **1**, 658 nm for **3**, and 634 nm for **4**. The observed transient absorption signals formed within the response time of the instrument (ca. 120 fs) and decayed monoexponentially with the lifetimes of 2.77 ± 0.02 ps for **1**, 632 ± 16 ps for **3**, and 570 ± 44 ps for **4**. The spectral and kinetic data are summarized in Table 4. On the basis of the kinetic behavior of these peaks (vide infra), the transient absorption near 650 nm was assigned to the excited singlet state of the bis(phenylethynyl)benzene chromophore.

The temporal evolution of the transient absorption spectra measured after 340 nm excitation of compounds **1**, **3**, and **4** is shown in Figure 6. Compounds **1** and **4** showed decay of the 650 nm transient with no consequent formation of any transient absorption in the spectral window of the instrument, and only model compound **3** contained another band at 600 nm formed concomitantly with the decay of the 650 nm band. The kinetics of the formation of the 600 nm absorption was not available since it overlapped substantially with the blue shoulder of the 658 nm peak.

Discussion

According to the commonly accepted mechanism of peroxide photodecomposition, initial excitation results in rapid cleavage of the oxygen−oxygen bond accompanied by loss of the carboxyl moiety forming carbon dioxide and the corresponding alkyl or aryl radical. Monitoring the formation of the carbon dioxide allows one to establish a time frame for the photoreaction and recognize two distinct stages—a series of early time events involving the formation of excited states and short-lived transient species and a later stage that corresponds to the evolution of the decarboxylated intermediates leading toward the final products.

Radical Intermediates Observed after Photolysis of Peroxy Esters. In TRIR experiments, we followed the kinetics of the

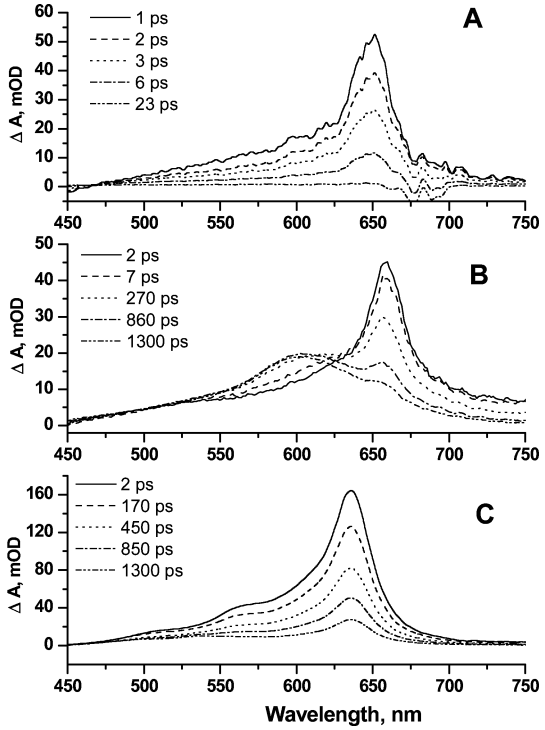

Figure 6. VIS transient spectra of **1**, **3**, and **4** acquired after the 340 nm laser pulse.

CHART 2: Structures of the Radical Intermediates (5 and 6) Formed after Photolysis of 1 and 2

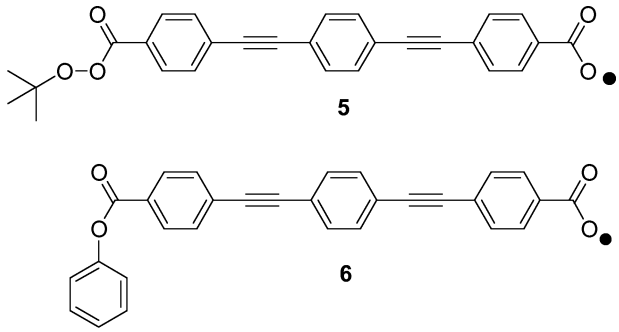

appearance of the carbon dioxide peak in **1** comparing its behavior with that of model compounds. As expected, photochemically stable model **3** shows no transient absorption around 2335 cm^{-1}. TRIR spectra of **1** and **2** each evidence the carbon dioxide peak as well as a transient absorption band centered at 2112 cm^{-1}. The analysis of kinetic traces at 2112 and 2335 cm^{-1} (Figure 1 and Table 1) revealed that, in both **1** and **2**, the decay of the transient signal at 2112 cm^{-1} was accompanied by a concomitant growth of the peak at 2335 cm^{-1}. This suggests that the transient absorbing at 2112 cm^{-1} is an immediate precursor of carbon dioxide. Neither the amplitude nor the decay time of the 2112 cm^{-1} transient signal changed when the solution was purged with oxygen instead of argon. This argues against assigning this peak to the triplet excited state or a carbon-centered radical, suggesting instead the presence of an oxygen-centered radical. On the basis of this, we assign the transient species absorbing at 2112 cm^{-1} to the carbonyloxyl radicals (**5** and **6**; see Chart 2) of bis(phenylethynyl)benzene.

We assign the frequency of 2112 cm^{-1} in **5** and **6** to stretching vibrations along the triple acetylene bond. While the ground-state spectra of **1** and **2** as a concentrated solution in $CHCl_3$ show a weak band around 2200 cm^{-1} corresponding to the

TABLE 5: Calculated Parameters of 4-Phenylethynylene Carbonyloxyl Radical of Different Symmetry and 4-Phenylethynylene Carboxylic Acid

sym	energy of the molecule, kcal/mol relative to $^2B_2$	IR freq of −C≡C− bond, cm^{-1} (scaled by 0.96[22])	IR intensity of −C≡C− bond
$^2B_1$	25.7	2126	998
$^2A_2$	14.0	2217	83
$^2A_1$	10.6	n/a	n/a
$^2B_2$	0.0	2217	107
acid (closed shell)	n/a	2220	42

−C≡C− stretch (Figure S3 and Figure S4 in SI), the 100 cm^{-1} red shift of the triple bond absorption in the aroyloxyl radical compared to the ground state indicates delocalization of the unpaired electron through the 1,4-bis(phenylethynyl)benzene chromophore sufficient to reduce the bond order of the triple bonds.

DFT calculations of the representative fragment of **5** and **6**, 4-phenylethynylene carbonyloxyl radical, were performed to analyze the electronic structure of the transient species observed. According to previous studies of aroyloxyl radicals, the lowest energy structure of these radicals would be expected to have $^2B_2$ orbital symmetry corresponding to a σ-type radical.[27] The free electron density in this radical is localized solely on the carboxy group and therefore has no ability to communicate with the π-system of the chromophore. DFT (UB3LYP 6-31G*) studies of the 4-phenylethynylene carbonyloxyl radical have shown that four possible structures of different orbital symmetry can exist (Table 5). The lowest energy structure possesses $^2B_2$ symmetry with the free electron occupying σ orbital on carboxy group (Figure 7). However, the vibrational analysis shows no −C≡C− frequency shift in the $^2B_2$ state compared to the closed shell system (Table 5).

An analysis of 4-phenylethynylene carbonyloxyl radical possessing $^2B_1$ symmetry revealed that the triple bond stretch shifted about 100 cm^{-1} to the red and the amplitude of this vibration increased (Table 5). These results correlate well with the experimental data obtained with the TRIR setup for **5** and **6**. The symmetry of the $^2B_1$ state determines the π nature of the radical, indicating that electron density of the single electron is delocalized through the whole π-system of the chromophore (Figure 7). The metastable $^2B_1$ geometry can be accessed after excitation of the starting material since it brings about an excess of 85 kcal/mol of energy while only 30 kcal/mol is needed to break the oxygen−oxygen bond.

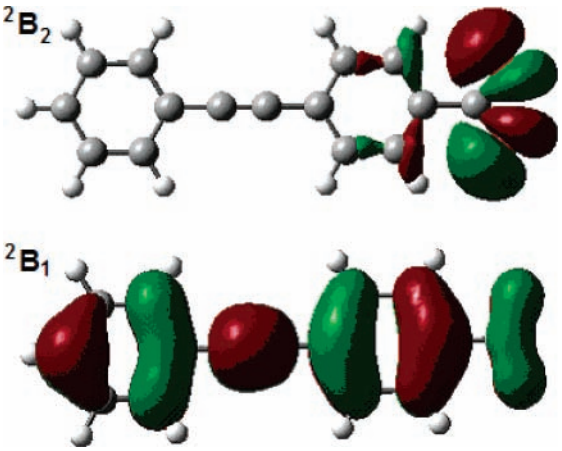

Figure 7. SOMO of $^2B_2$ and $^2B_1$ states of the 4-phenylethynylene carbonyloxyl radical.

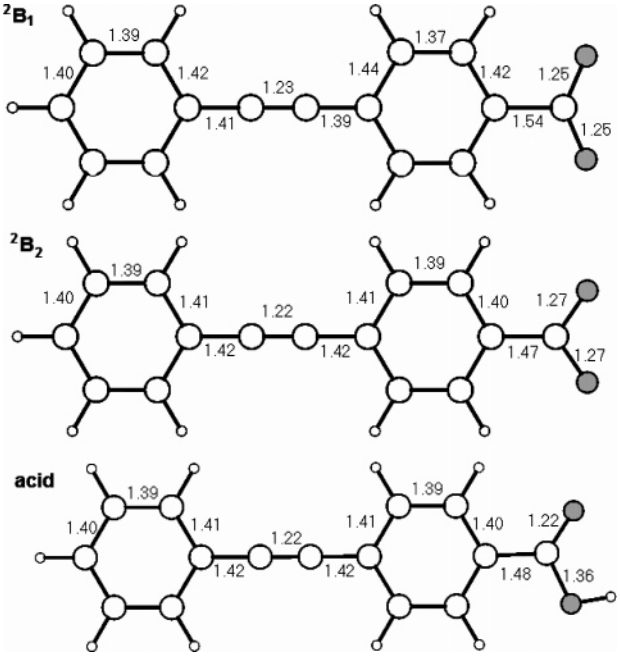

Figure 8. Optimized geometry of the $^2B_1$ and $^2B_2$ states of the 4-phenylethynylene carbonyloxyl radical and 4-phenylethynylene carboxylic acid.

CHART 3: Hybrid Resonance Structure of 5 and 6 Demonstrating Delocalization of the Free Electron

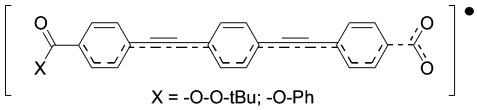

The $^2A_2$ state of 4-phenylethynylene carbonyloxyl radical also has π nature. However, it does not demonstrate the reduction in the triple bond order (Table 5). The σ $^2A_1$ was found to have an unstable configuration with respect to decarboxylation of the radical since several imaginary frequencies were found for this geometry. All efforts to find a stable configuration of the $^2A_1$ led to convergence to the $^2B_2$ or a failure to find a minimum in potential energy.

A bond length analysis shows an increase in the triple bond length and decrease in bond lengths of the adjacent single bonds compared to the closed-shell analogue (carboxylic acid) for the $^2B_1$ radical only. The $^2B_2$ radical does not evidence this effect (Figure 8).

On the basis of the observed structural changes in the phenylene−ethynylene chromophore upon formation of the $^2B_2$ aroyloxyl radical, a cumulene-like structure (Chart 3) can be proposed. The fully developed cumulene structure would be expected to have an intense absorption[8] around 1950 cm^{-1} which places the structure of **5** and **6** between localized acetylene and completely cumulene structures.

The effect of an unpaired electron on the bis(phenylethynyl)-benzene chromophore appears to be similar to the electronic excitation of the parent molecule to the singlet excited state. A similar shift (from 2217 cm^{-1} in the ground state to 2128 cm^{-1} in S_1) was observed in the absorption of the −C≡C− bond upon excitation to S_1 as measured by time-resolved resonance Raman spectroscopy;[8] this shift was attributed to the partially reduced triple bond order in S_1.

Triplet Excited State of the 1,4-Bis(phenylethynyl)benzene Chromophore. Regardless of the photochemical stability of **3**, a ground-state bleaching signal was anticipated due to the formation of excited states. The increase in laser power from

TABLE 6: FTIR Vibrational Frequencies of 3 in the Electronically Ground and in the Lowest Triplet Excited States

electronic state	obsd freq,[a] cm^{-1}	calcd freq,[b] cm^{-1}
ground state (S_0)	1735,[c] 1610[d]	1750,[c] 1590[d]
triplet state (T_1)	1712[c,e]	1728,[c] 1503[d]
spectral shift (TS − GS)	−23[c]	−22,[c] −87[d]

[a] IR frequencies measured in steady state and time-resolved FTIR experiments. [b] IR frequencies calculated with B3LYP/6-31G(d) level/basis set and scaled by factor 0.96.[22] [c] Carbonyl stretch. [d] Phenyl C−C stretch. [e] The direct observation of the phenyl C−C stretch in the triplet excited state was not possible due to limited spectral window of the TRIR setup.

1.5 to 5 mJ/pulse allowed the observation of a bleaching of the ground state at 1735 cm^{-1} together with a new transient absorption band red shifted by ca. 20 cm^{-1} (Figure 3). Also, a bleaching at 1604 cm^{-1} corresponding to the ground-state absorption band associated with the C−C stretch of the phenyl ring[28] was observed. Bleaching and absorption returned to the baseline with a similar time constant (Table 2). The transients observed in TRIR experiments with **3** were assigned to the triplet state absorption on the basis of their spectral and kinetic behavior and DFT calculations. A calculated shift (23 cm^{-1}) of the carbonyl group vibration from the ground to the lowest triplet excited state agrees well with the experimental data (Table 6). Notably, the predicted shift of the phenyl C−C stretch is four times greater than that of the carbonyl vibration shift. This indicates an electron density in the triplet excited state is delocalized mostly through the central bis(phenylethynyl)-benzene chromophore partially reducing the bond order (energy) of the C−C bond and driving the infrared absorption to lower frequencies. The carbonyl groups are involved in the overall energy redistribution and show the red shift of the absorption due to a partial electron donation from the central chromophore. This observation supports the conclusions drawn previously about redistribution of the electron density in compounds containing bis(phenylethynyl)benzene chromophore leading to the formation of a cumulene-like structures.[9,29]

The lifetime of the triplet state observed by TRIR was significantly shorter than the lifetime measured in the TRUV experiment. The intrinsically lower extinction coefficients in the infrared region of the spectrum compared to the VIS region require higher concentrations of the transient species (e.g. higher concentrations of the starting materials and higher laser power), thus increasing the probability of the bimolecular interactions such as triplet−triplet annihilation.

Time-resolved UV−vis (TRUV) spectra of **1** and **3** (Figure 4) show a common broad transient around 550 nm. A substantially longer lifetime and sensitivity to dissolved oxygen (Table 3) unambiguously suggest its assignment to the triplet excited state of the bis(phenylethynyl)benzene chromophore.

The transient absorption band acquired for **1** resembles mostly the spectral features of **3** with no additional transients corresponding to the absorption of radical species. Due to the spectral overlap, the triplet−triplet excited-state absorption can be distinguished from the absorption of radical species on the basis of the difference in transient behavior between peroxy ester **1** and model **3** (see the kinetic data in Table 3). The transient absorption after photolysis of **1** decays biexponentially with a short-lived component similar to that of the aroyloxyl radical measured in the TRIR experiment and another component similar to lifetime observed in **3**. The sensitivity of short-lived transient to the radical quencher, acrylonitrile, supports the assignment of this component to the carbonyloxyl radical. The

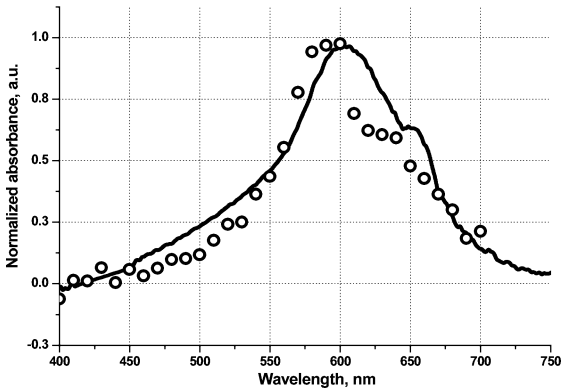

Figure 9. Spectral overlay of the T_1-T_n transient absorption bands acquired 1.3 ns (line, from ultrafast experiment) and 3 μs (circles, nanosecond experiment) after excitation of **3**.

deconvoluted spectrum of **5** demonstrates broad transient absorption with maximum above 800 nm, typical for aroyloxyl radicals. The absorption of **5** is considerably lower than that of the triplet state indicating that extinction coefficient of the latter is significantly higher than that of the radical.

Ultrafast Studies of the Excited States of 1,4-Bis(phenylethynyl)benzene Chromophore. Ultrafast VIS spectra of **1**, **3**, and **4** are similar, featuring a characteristically sharp band around 650 nm and a slight red shift as the conjugation increases due to the addition of more electron rich substituents (Figure 5). The similar transient spectra of **1**, **3**, and **4** indicate that the 650 nm absorption band is due to the excited state of the chromophore rather than absorption of photodecomposition products of **1**, since **3** and **4** possess little reactivity under the experimental conditions.

The 650 nm absorption forms faster than 100 fs and decays, in the case of **4**, with a lifetime similar to that reported previously for fluorescence decay of 1,4-bis(phenylethynyl)-benzene[7,30] suggesting assignment to the absorption of the singlet excited state.

The addition of the peroxide functionality to the bis-(phenylethynyl)benzene core (**1**) has a small effect on the maximum position but dramatically changes the lifetime of the singlet exited state, decreasing it about 200 times compared to **3**. Thus, the rupture of the weak oxygen−oxygen bond in **1** causes a drastic change in the observed lifetime of S_1. Accordingly, oxygen−oxygen bond cleavage is the dominant pathway for deactivation of the singlet excited-state population of **1** at a rate of 3.6×10^{11} s^{-1}.

The time evolution of the transient absorption in **3** shows that species absorbing at 600 nm are the direct successors of the singlet excited state (Figure 6). Direct comparison of the transients detected in ultrafast experiments with spectral data obtained on the longer time scale clearly show that species detected 1.3 ns and 3 μs after the laser pulse have the same origin (Figure 9).

Mechanism of Decomposition of 1. No distinctive signal associated with triplet excited-state absorption was observed on the ultrafast time scale in **1** though the rate of the intersystem crossing in **1** is expected to be similar to that of **3** (2.8×10^8 s^{-1}). The only two channels of the excited-state deactivation in model compound **3** are assumed—the fluorescence and intersystem crossing to the triplet excited state. The fluorescence quantum yield measured for **3** was 0.82. Thus, the quantum yield of the triplet state formation in **3** (Φ_T) is 0.18. The rate of the intersystem crossing can be calculated from the observed

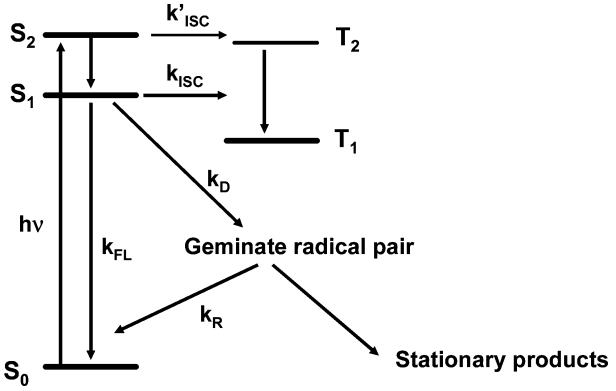

Figure 10. Energy level diagram showing the excitation energy ($h\nu$) redistribution in **1**. The rate constants are labeled as follows: k_{FL}, fluorescence; k'_{ISC}, intersystem crossing from higher singlet excited state; k_{ISC}, intersystem crossing from S_1 state; k_D, dissociation of the oxygen−oxygen bond; k_R, recombination of the geminate radical pair.

rate of the singlet excited-state decay ($k_{obs} = 1.58 \times 10^9\ s^{-1}$):

$$k_{ISC} = \Phi_T k_{obs} = 2.8 \times 10^8\ s^{-1}$$

Assuming that the triplet state in **1** is formed exclusively from the S_1 the quantum yield of the triplet state formation in **1** can be found as

$$\Phi'_T = k_{ISC}/k'_{obs} = 0.8 \times 10^{-3}$$

where k'_{obs} is the observed rate of the singlet excited-state decay in **1**.

Thus the ratio of the quantum yields of the triplet state formation in **3** relative to **1** is:

$$\Phi_T/\Phi'_T = 225$$

However, the ratio of the amplitudes of T_1-T_n absorption obtained from nanosecond TRUV experiments (see Table 3) with **3** and **1** only equals 1/8 (0.08/0.65). This suggests another channel for the formation of the triplet excited state in addition to intersystem crossing from the S_1 state. Biswas et al.,[31] in studies of bis(phenylethynyl)benzene and its analogues, suggested the presence of several low-lying singlet states accessed by the excitation pulse. On the basis of steady-state and time-resolved fluorescence measurements, the authors proposed a $S_n-T_n-T_1$ population pathway for the lowest triplet state. The same approach can be used to explain the energy flow between electronic levels in **1** (Figure 10) resulting in the higher ratio of the triplet state quantum yields in **1** and **3**.

Finally, we discuss the quantum efficiency of the photochemical channel in **1**. The ratio of the quantum yields of the triplet state formation in **3** (Φ_T) relative to **1** (Φ'_T) was determined from nanosecond TRUV experiments as the ratio of the amplitudes of the triplet state absorption ($\Phi_T/\Phi'_T = 8$). The value of Φ_T was found to be 0.18 (see above); thus, the Φ'_T should equal to 0.02. The fluorescence quantum yield of **1** was found to be around 0.03. As the fluorescence and the triplet state formation are the only expected pathways of the excitation energy redistribution besides the chemical reaction, the quantum yield of the oxygen−oxygen bond dissociation is expected to be 0.95. However, the photodecomposition quantum of **1** yield measured directly was only 60%. This difference implies the presence of a geminate pair recombination pathway within the solvent cage which re-forms the starting material. Such an effect is not uncommon in decomposition of peroxides, and the ^{18}O labeling experiments by Taylor et al.[32] demonstrated that thermal decomposition of acetyl peroxide was followed by recombination of acetoxy radicals within the solvent cage yielding 38% of the initial peroxide. Viscosity dependence studies have also confirmed a significant contribution of the cage recombination to the decomposition rate of perfluorinated acyl peroxides.[33]

We monitored the disappearance of **1** in hexane and mineral oil (Nujol) solutions by IR spectroscopy after irradiation with 325 nm light. The photodecomposition quantum yield of **1** in hexane (viscosity = 0.3 cP) was found to be twice that in Nujol (viscosity = 67 cP). The similar polarities of hexane and Nujol ensure that polarity effect is eliminated. The dependence of photodecomposition quantum yield of **1** on viscosity clearly demonstrates the significance of cage effect in recovery of the starting material.

Studies of the dissociation dynamics of small molecules show that primary recombination of the geminate radical pair can occur as fast as several hundreds of femtoseconds,[34] which is significantly faster that diffusion rate ($\sim 10^{10}\ s^{-1}$) and rate of the decarboxylation of the aroyloxyl radical ($\sim 5 \times 10^6\ s^{-1}$). We, therefore, assume that recombination of the radicals within the solvent cage successfully competes with diffusion and decarboxylation resulting in only 60 % of dissociated molecules to escape the solvent cage while the remainder recombines to give vibrationally excited ground state.

Conclusions

The addition of peroxy ester functionality on 1,4-bis-(phenylethynyl)benzene termini dramatically increases the rate of singlet excited state decay, due to extremely fast cleavage of the peroxy bond ($3.6 \times 10^{11}\ s^{-1}$) leading to the formation of aroyloxyl radicals. The infrared spectrum of these radicals shows red shift in the triple bond vibration frequency compared to the ground state which is indicative of a decrease in the −C≡C− bond order due to redistribution of the electron density. This clearly shows that the unpaired electron is partially delocalized through the conjugated backbone of the chromophore and brings some cumulene-like character to the structure causing changes similar to electronic excitation of the parent chromophore. The DFT calculations reveal that observed shift takes place only for radicals possessing $^2B_1$ symmetry, while radicals with other symmetries ($^2B_2$, $^2A_2$) as well as closed-shell analogues do not demonstrate this shift.

The proposed photodecomposition mechanism is based on the rates of photophysical and photochemical channels and involves an additional population channel of the 1,4-bis-(phenylethynyl)benzene triplet excited state from the upper singlet states.

The significant influence of recombination of radical species formed within the solvent cage was observed from the estimated quantum efficiencies of −O−O− bond cleavage and confirmed experimentally by measuring photodecomposition quantum yields in solvents of different viscosities. This observation was found to be consistent with formation of a singlet diradical pair from the singlet excited state of the starting material.

Acknowledgment. We thank Dr. John Cable for fruitful discussions. The Ohio Laboratory for Kinetic Spectrometry is gratefully acknowledged for providing equipment for transient spectroscopy measurements. D.E.P. is grateful to the McMaster Endowment for support in the form of a Fellowship.

Supporting Information Available: Kinetic details of TRIR experiments with **1** and **2**, FTIR spectra of **1** and **2**, the Cartesian

coordinates and vibrational frequencies of optimized geometry of the 4-phenylethynylene carbonyloxyl radical of $^2B_1$ and $^2B_2$ symmetries, 4-phenylethynylene carboxylic acid, and the ground and lowest triplet excited states of **3**. This material is available free of charge via the Internet at http://pubs.acs.org.

References and Notes

(1) Center for Photochemical Sciences Contribution No. 577.

(2) Englert, B. C.; Smith, M. D.; Hardcastle, K. I.; Bunz, U. H. F. *Macromolecules* **2004**, *37*, 8212−8221.

(3) For example see: (a) Kawabata, S.; Yamazaki, I.; Nishimura, Y.; Osuka, A. *J. Chem. Soc., Perkin Trans. 2* **1997**, 479−484. (b) Atienza, C.; Insuastry, B.; Seoane, C.; Martin, N.; Ramey, J.; Rahman, G. M. A.; Guldi, D. M. *J. Mater. Chem.* **2005**, *15*, 124−132.

(4) Zhan, X.; Yang, M.; Xu, M.; Liu, X.; Ye, P. *Macromol. Rapid Commun.* **2001**, *22*, 358−362.

(5) Meier, H.; Ickenroth, D.; Stalmach, U.; Koynov, K.; Bahtiar, A.; Bubeck, C. *Eur. J. Org. Chem.* **2001**, 4431−4443.

(6) For example see: (a) Levitus, M.; Garcia-Garibay, M. A. *J. Phys. Chem.* **2000**, *104*, 8632−8637. (b) Levitus, M.; Schmieder, K.; Ricks, H.; Shimizu, K. D.; Bunz, U. H. F.; Garcia-Garibay, M. A. *J. Am. Chem. Soc.* **2001**, *123*, 4259−4265.

(7) Beeby, A.; Findlay, K.; Low, P. J.; Marder, T. B. *J. Am. Chem. Soc.* **2002**, *124*, 8280−8284.

(8) Beeby, A.; Findlay, K.; Low, P. J.; Marder, T. B.; Matousek, P.; Parker, A. W.; Rutter, S. R.; Towrie, M. *Chem. Commun.* **2003**, 2406−2407.

(9) Sluch, M. I.; Godt, A.; Bunz, U. H. F.; Berg, M. A. *J. Am. Chem. Soc.* **2001**, *123*, 6447−6448.

(10) Polyansky, D. E.; Neckers, D. C. *J. Phys. Chem. A* **2005**, *109*, 2793−2800.

(11) Falvey, D. E.; Schuster, G. B. *J. Am. Chem. Soc.* **1986**, *108*, 7419−7420.

(12) Aschenbru1cker, J.; Buback, M.; Ernsting, N. P.; Schroeder, J.; Steegmu1ller, U. *J. Phys. Chem. B* **1998**, *102*, 5552−5555.

(13) Wang, J.; Itoh, H.; Tsuchiga, M.; Tokumaru, K.; Sakuragi, H. *Tetrahedron* **1995**, *51*, 11967−11977.

(14) Rusakowicz, R.; Testa, A. C. *J. Phys. Chem.* **1968**, *72*, 2680−2681.

(15) Melhuish, W. H. *J. Phys. Chem.* **1961**, *65*, 229−235.

(16) Perrin, D. D.; Armarego, W. L. F. *Purification of Laboratory Chemicals*; Butterworth Heinemann: Oxford, U.K., 1994.

(17) Fedorov, A. V.; Danilov, E. O.; Merzlikine, A. G.; Rodgers, M. A. J.; Neckers, D. C. *J. Phys. Chem. A* **2003**, *107*, 3208−3214.

(18) Merzlikine, A. G.; Voskresensky, S. V.; Danilov, E. O.; Fedorov, A. V.; Rodgers, M. A. J.; Neckers, D. C. *Photochem. Photobiol. Sci.* **2004**, *3*, 892−997.

(19) Gentili, P. L.; Danilov, E.; Ortica, F.; Rodgers, M. A. J.; Favaro, G. *Photochem. Photobiol. Sci.* **2004**, *3*, 886−891.

(20) Frisch, M. J.; et al. *Gaussian 98*, revision A.7; Gaussian, Inc.: Pittsburgh, PA, 1998.

(21) Foresman, J. B.; Frisch, A. *Exploring Chemistry with Electronic Structure Methods*; Gaussian: Pittsburgh, PA, 1996.

(22) Singh, A.; Andrews, L. J.; Keefer, R. M. *J. Am. Chem. Soc.* **1962**, *84*, 1179.

(23) Corey, E. J.; Fuchs, P. L. *Tetrahedron Lett.* **1972**, 3769.

(24) Hwang, G. T.; Son, H. S.; Ku, J. K.; Kim, B. H. *J. Am. Chem. Soc.* **2003**, *125*, 11241−11248.

(25) Shim, W., II; Risen, W. M. *J. Organomet. Chem.* **1984**, *260*, 171−180.

(26) Drefahl, G.; Plotner, G. *Chem. Ber.* **1958**, *91*, 1280−1285.

(27) Feller, D.; Huyser, E. S.; Borden, W. T.; Davidson, E. R. *J. Am. Chem. Soc.* **1983**, *105*, 1459−1466.

(28) Silverstein, R. M.; Webster, F. X. *Spectrometric Identification of Organic Compounds*; John Willey & Sons. Inc.: New York, 1998.

(29) Schmieder, K.; Levitus, M.; Dang, H.; Garcia-Garibay, M. A. *J. Phys. Chem. A* **2002**, *106*, 1551−1556.

(30) Birckner, E.; Grummt, U.-W.; Goeller, A. H.; Pautszch, T.; Egbe, D. A.; Al-Higari, M.; Klemm, E. *J. Phys. Chem. A* **2001**, *105*, 1037.

(31) Biswas, M.; Nguyen, P.; Marder, T. B.; Khundkar, L. R. *J. Phys. Chem. A* **1997**, *101*, 1689−1695.

(32) Taylor, J. W.; Martin, J. C. *J. Am. Chem. Soc.* **1996**, *88*, 3650−3651.

(33) Bunyard, W. C.; Kadla, J. F.; DeSimone, J. M. *J. Am. Chem. Soc.* **2001**, *123*, 7199−7206.

(34) Schwartz, B. J.; King, J. C.; Zhang, J. Z.; Harris, C. B. *Chem. Phys. Lett.* **1993**, *203*, 503−508.